

Article

# Immobilization of Ionic Liquid on a Covalent Organic Framework for Effectively Catalyzing Cycloaddition of CO<sub>2</sub> to Epoxides

Qianqian Yan <sup>1,†</sup>, Hao Liang <sup>1,†</sup>, Shenglin Wang <sup>1</sup>, Hui Hu <sup>1</sup>, Xiaofang Su <sup>1,\*</sup>, Songtao Xiao <sup>2,\*</sup>, Huanjun Xu <sup>3</sup>, Xuechao Jing <sup>4</sup>, Fei Lu <sup>1</sup> and Yanan Gao <sup>1,\*</sup> 

<sup>1</sup> Key Laboratory of Ministry of Education for Advanced Materials in Tropical Island Resources, Hainan University, No. 58, Renmin Avenue, Haikou 570228, China

<sup>2</sup> China Institute of Atomic Energy, Beijing 102413, China

<sup>3</sup> School of Science, Qiongtai Normal University, Haikou 571127, China

<sup>4</sup> Liaocheng Luxi Polycarbonate Co., Ltd., Liaocheng 252000, China

\* Correspondence: [sxf@hainanu.edu.cn](mailto:sxf@hainanu.edu.cn) (X.S.); [xiao200112@163.com](mailto:xiao200112@163.com) (S.X.); [ygao@hainanu.edu.cn](mailto:ygao@hainanu.edu.cn) (Y.G.)

† These authors contributed equally to this work.

**Abstract:** Transforming CO<sub>2</sub> into value-added chemicals has been an important subject in recent years. The development of a novel heterogeneous catalyst for highly effective CO<sub>2</sub> conversion still remains a great challenge. As an emerging class of porous organic polymers, covalent organic frameworks (COFs) have exhibited superior potential as catalysts for various chemical reactions, due to their unique structure and properties. In this study, a layered two-dimensional (2D) COF, IM4F-Py-COF, was prepared through a three-component condensation reaction. Benzimidazole moiety, as an ionic liquid precursor, was integrated onto the skeleton of the COF using a benzimidazole-containing building unit. Ionization of the benzimidazole framework was then achieved through quaternization with 1-bromobutane to produce an ionic liquid-immobilized COF, i.e., BMIM4F-Py-COF. The resulting ionic COF shows excellent catalytic activity in promoting the chemical fixation of CO<sub>2</sub> via reaction with epoxides under solvent-free and co-catalyst-free conditions. High porosity, the one-dimensional (1D) open-channel structure of the COF and the high catalytic activity of ionic liquid may contribute to the excellent catalytic performance. Moreover, the COF catalyst could be reused at least five times without significant loss of its catalytic activity.

**Keywords:** covalent organic framework; ionic liquid; carbon dioxide; catalysis; cyclic carbonates



**Citation:** Yan, Q.; Liang, H.; Wang, S.; Hu, H.; Su, X.; Xiao, S.; Xu, H.; Jing, X.; Lu, F.; Gao, Y. Immobilization of Ionic Liquid on a Covalent Organic Framework for Effectively Catalyzing Cycloaddition of CO<sub>2</sub> to Epoxides. *Molecules* **2022**, *27*, 6204. <https://doi.org/10.3390/molecules27196204>

Academic Editor: Boiko Cohen

Received: 22 August 2022

Accepted: 16 September 2022

Published: 21 September 2022

**Publisher's Note:** MDPI stays neutral with regard to jurisdictional claims in published maps and institutional affiliations.



**Copyright:** © 2022 by the authors. Licensee MDPI, Basel, Switzerland. This article is an open access article distributed under the terms and conditions of the Creative Commons Attribution (CC BY) license (<https://creativecommons.org/licenses/by/4.0/>).

## 1. Introduction

Covalent organic frameworks (COFs) are an emerging class of porous crystalline polymers formed through the linkage of organic building units via strong covalent bonds [1–4]. They feature a large surface area, highly ordered porosity, designable topological structure and easy modification, making them intriguing materials for various applications, such as catalysis [5–11], gas adsorption/separation [12–16], energy storage [17–19] and environmental remediation [20–24]. In the catalysis field, the flexible regulation of the pore environment (i.e., pore size, shape and size distribution) and large numbers of structural topologies offer more possibilities for creating new patterns of catalytic reactivity. In addition, one-dimensional (1D) open channels found in COFs enable the rapid diffusion of substances to promote catalytic reactions. In contrast to traditional porous materials such as activated carbon and zeolites, well-defined catalytic active sites can be spatially separated within the framework, and the number of catalytic sites can be controlled precisely in the desired manner [25,26]. Furthermore, due to the organic nature of COFs, they can be easily modified through either a bottom-up strategy or a post-synthetic modification strategy. As such, the use of COFs as catalysts or catalyst carriers has developed rapidly over recent

years. A variety of catalytic active moieties involving metal ions or nanoparticles, as well as a variety of organocatalysts, have been successfully immobilized onto the skeletons of COFs; the resulting COFs exhibited good catalytic performance in many reactions, such as the Heck reaction [27], the Michael addition reaction [28], the Henry reaction [29], Suzuki–Miyaura coupling [6] and the Diels–Alder reaction [30]. In addition, COFs have been used as a multifunctional catalyst for cascade reactions, such as the Heck-epoxidation tandem reaction [31], the oxidation-Knoevenagel cascade reaction [32] and the addition-oxidation cascade reaction [33].

The greenhouse effect is an important cause of global warming; among various greenhouse gases, CO<sub>2</sub> is the most frequently implicated in global warming, but is also the most abundant carbon feedstock [34]. In recent years, considerable efforts have been devoted to transforming CO<sub>2</sub> into useful chemicals. Among various value-added chemicals, cyclic carbonates are an important class of chemical products that have been widely used as polar aprotic solvents, electrolytes for lithium-ion batteries, monomers in polymeric materials and fine-chemical intermediates [35–37]. To this end, various catalysts have been developed for the highly effective transformation of CO<sub>2</sub> into cyclic carbonates, including Schiff bases [38], Salen complexes [39] and metalloporphyrins [40]. Moreover, ionic liquids, including ammonium [41,42], phosphonium [43], imidazolium [44,45] and pyridinium salts [46], have been successfully applied to catalyze the cycloaddition of CO<sub>2</sub> to epoxides. However, as homogeneous catalysts, ionic liquids are difficult to separate from the reaction system, which limits their practical application on a large scale. For this reason, ionic liquids have been immobilized onto different supports, such as porous silicas [47,48], polymers [49] and metal-organic frameworks used as heterogeneous catalysts for easy product separation [50].

The immobilization of ionic liquids on COFs would combine the unique properties of COFs, such as large surface area, controlled porosity, a 1D open-channel structure and the high catalytic activity of ionic liquids, in one material [51–53]. In addition, confining ionic liquids within a special pore environment may afford chemical reactions with shape-, size-, chemo- or enantio-selectivity. In order to further explore the potential of ionic liquids immobilized on COFs in heterogeneous catalysis, we here describe a post-synthetic strategy for the immobilization of ionic liquids on the channel walls of a 2D COF, IM4F-Py-COF. The resulting ionic liquid-containing COF (BMIM4F-Py-COF) exhibited excellent catalytic performance regarding the cycloaddition of CO<sub>2</sub> to epoxides. Furthermore, good recyclability was observed for the ionic liquid-immobilized COF catalyst.

## 2. Experimental

### 2.1. Materials

The building units 4,4',4'',4'''-(Pyrene-1,3,6,8-tetrayl) tetraaniline (PyTTA), 5,6-bis(4-formylbenzyl)-1-methyl-1H-benzimidazole (IM) and 2',3',5',6'-tetrafluoro-[1,1':4',1''-terphenyl]-4,4'-dicarbaldehyde (4F) were synthesized in accordance with the reported procedures [54,55]. All starting materials and solvents, unless otherwise specified, were obtained from commercial resources and used without further purification.

### 2.2. Synthesis of IM4F-Py-COF

IM4F-Py-COF was synthesized following the previously reported protocol [56]. In a typical procedure, PyTTA (21.67 mg, 0.04 mmol), 4F (14.32 mg, 0.04 mmol) and IM (13.76 mg, 0.04 mmol), as well as 2 mL of 1,2-dichlorobenzene, were charged into a 10 mL glass ampule vessel. The mixture was sonicated for 10 min, and 0.2 mL of 6.0 M acetic acid was rapidly added. The vessel was flash-frozen in liquid nitrogen and degassed by three freeze–pump–thaw cycles. The internal pressure of the vessel was decreased to below 5 Pa and the vessel was rapidly flame-sealed. The reaction was carried out at 120 °C for 3 days. The precipitate was separated and washed thoroughly with anhydrous THF and acetone, successively, and dried at 100 °C overnight under vacuum to produce a yellow powder in a 78% yield. Elemental analysis: for C<sub>82</sub>H<sub>48</sub>F<sub>4</sub>N<sub>6</sub>: Calcd. C, 82.52%; H, 4.03%; N, 7.04%. Found: C, 76.11%; H, 4.75%; N, 6.05%.

### 2.3. Synthesis of BMIM4F-Py-COF

The ionization of IM4F-Py-COF into BMIM4F-Py-COF was achieved through a quaternization process. To a 50 mL round-bottom flask were added 50 mg of IM4F-Py-COF, 5 mL of 1-bromobutane and 20 mL of acetonitrile. The reaction was heated under reflux at 80 °C for 24 h. After cooling to room temperature, the precipitate was collected by filtration and washed thoroughly with anhydrous ethanol and acetone, successively. The powder was dried at 100 °C overnight under vacuum to give a dark yellow product in a 95% yield.

### 2.4. General Procedures for Cycloaddition of CO<sub>2</sub> with Epoxides

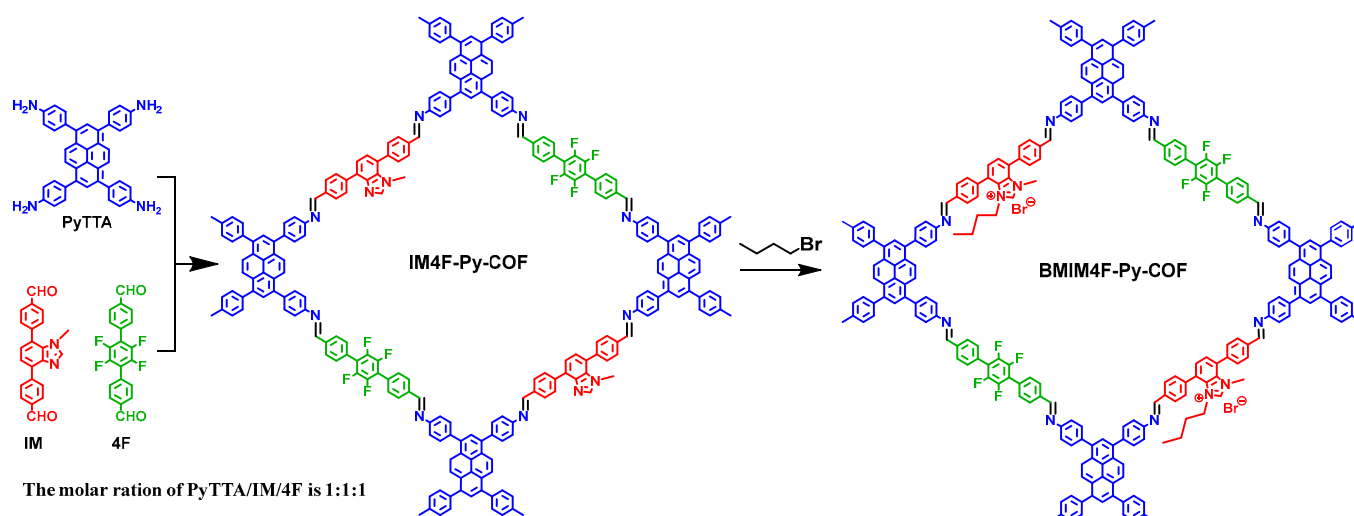
The reactions were carried out in a 25 mL sealed Teflon-lined autoclave. Firstly, 3.8 mmol epoxide and 20 mg BMIM4F-Py-COF were charged into the reactor without solvent. The air in the autoclave was then removed by a CO<sub>2</sub> purge. The autoclave was pressurized up to a desired pressure (generally 4.0 MPa) with CO<sub>2</sub> and the temperature was raised to 110 °C. The reaction was conducted for 12 h. After the reaction, a small amount of the resultant reaction mixture was sampled from the autoclave for nuclear magnetic resonance (NMR) analysis in order to quantitatively evaluate the conversion of epoxide. The crude product was filtered and purified using column chromatography. The isolated yield was calculated based on the weight of the obtained product.

### 2.5. Characterization

Power X-ray diffraction (PXRD) measurements were recorded on a PANalytical X'Pert model Pro Multipurpose Diffractometer (Davis, CA, USA) using Cu K<sub>α</sub> radiation at 40 kV and 40 mA. The signals were collected from 2θ of 2.5–40° at 0.03° step scan with exposure time of 10 s per step. Nitrogen sorption isotherms were measured volumetrically at 77 K using a Quantachrome Autosorb-iQ2 analyzer (Quantachrome Instruments, Boynton Beach, FL, USA) with ultra-high-purity gases. The fresh samples were activated at 100 °C for 15 h under high vacuum prior to analysis. The Brunauer–Emmett–Teller (BET) model was used to determine the specific surface areas using desorption branches over  $P/P_0$  of 0.01–0.05. In all isotherm plots, closed circles describe adsorption data points and open circles are used to represent desorption data points. The pore size distribution was evaluated by the nonlocal density function theory (NLDFT) method. <sup>1</sup>H and nuclear magnetic resonance (NMR) spectra were recorded by a Bruker Advance III 400 MHz NMR spectrometer (Bruker BioSpin Corporation, Fällanden, Switzerland). Gas chromatography (GC, Agilent 7890A, Agilent, Palo Alto, CA, USA) equipped with a capillary column (HP-5, 30 m × 0.25 mm) using a flame ionization detector was carried out. The Br<sup>−</sup> content in the COFs was measured by ion chromatography, which was carried out with a Dionex ICS 1100 instrument with suppressed conductivity detection. Elemental analysis was performed using an organic elemental analyzer (vario MACRO cube, Elementar, Langenselbold, Germany). Fourier-transform infrared (FT-IR) spectra were recorded using KBr pellets on a Bruker model TENSOR 27 spectrophotometer. Thermogravimetric analysis (TGA, STA449F3, NETZSCH, Selb, Germany) was performed by heating from room temperature to 800 °C at a rate of 10 °C min<sup>−1</sup> with a N<sub>2</sub> flow rate of 20 mL min<sup>−1</sup>.

## 3. Results and Discussion

The IM4F-Py-COF precursor was first prepared through the condensation reaction of four-branched 4,4',4'',4'''-(pyrene-1,3,6,8-tetrayl) tetraaniline (PyTTA) and linear 5,6-bis(4-formylbenzyl)-1-methyl-1H-benzimidazole (IM) and 2',3',5',6'-tetrafluoro-[1,1':4',1''-terphenyl]-4,4'-dicarbaldehyde (4F) at a molar ratio of 1:1:1 [56]. The fluoro-containing building unit 4F was introduced into the COF to enhance the interlayer interaction that favors the formation of high crystallization and large porosity in COFs [57]. Ionization was achieved through the quaternization reaction with 1-bromobutane to give an ionic COF product, BMIM4F-Py-COF (Scheme 1).



**Scheme 1.** Synthesis procedure of BMIM4F-Py-COF.

The crystallinity of the IM4F-Py-COF was characterized by powder X-ray diffraction (PXRD), as shown in Figure 1. IM4F-Py-COF exhibited several strong diffraction peaks, observed at  $2.8^\circ$ ,  $3.8^\circ$ ,  $5.5^\circ$ ,  $8.2^\circ$ ,  $10.9^\circ$ ,  $13.7^\circ$  and  $23.2^\circ$ , which can be attributed to the (110), (020), (220), (330), (400), (550) and (001) facets, respectively. The crystalline structure of the COF was analyzed based on the PXRD pattern together with the computational simulation. Given the connectivity and structure of the building blocks, an eclipsed AA stacking model and a staggered AB model were considered. It was found that the AA stacking model reproduced the PXRD pattern well (Figure 1, black, red and blue curves). The final lattice parameters were extracted as  $a = 49.83 \text{ \AA}$ ,  $b = 42.59 \text{ \AA}$ ,  $c = 3.93 \text{ \AA}$  and  $\alpha = 89.50^\circ$ ,  $\beta = 88.71^\circ$ ,  $\gamma = 90.06^\circ$  after Pawley refinement (Table S1), confirming the peak assignment, as evidenced by the negligible difference (Figure 1, magenta curve). We excluded the possibility of a staggered AB model because the simulated PXRD pattern did not match the observed data (Figure 1, green curve). After the ionization, the produced BMIM4F-Py-COF showed an identical PXRD pattern to that of the precursor IM4F-Py-COF, suggesting that both COFs had similar crystal structures (Figure S1).

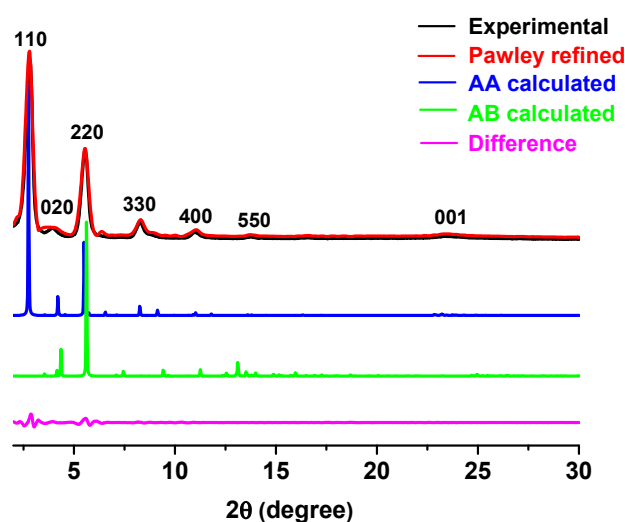


**Figure 1.** PXRD patterns of IM4F-Py-COF. Experimental pattern (black), profiles simulated using the Pawley refinement (red), the difference between experimental and refined patterns (magenta), AA-stacking (blue) and AB-stacking (green) modes of the IM4F-Py-COF.

The formation of an imine-linked COF was further confirmed by an FT-IR spectrum (Figure 2). A new peak observed at  $1622\text{ cm}^{-1}$  for IM4F-Py-COF and BMIM4F-Py-COF was ascribed to the characteristic peak of the imine ( $-\text{C}=\text{N}-$ ) group. In addition, the solid-state  $^{13}\text{C}$  cross-polarization/magic-angle spinning (CP/MAS) NMR spectrum of IM4F-Py-COF and BMIM4F-Py-COF demonstrated a signal at  $150.0\text{ ppm}$  (Figure S2), which was assigned to the carbon atoms of imine linkages, further confirming the imine linkage of the COFs. The ionization of IM4F-Py-COF into BMIM4F-Py-COF was confirmed by the appearance of a new peak at  $2956\text{ cm}^{-1}$  in BMIM4F-Py-COF (Figure 2), which was ascribed to the characteristic stretching of  $-\text{CH}_2-$ , indicating the successful grafting of n-butyl groups onto the skeleton of the IM4F-Py-COF. Excessive ionization of the COF skeleton would destroy the crystalline structure of the COF, so the quaternization reaction time was set for 24 h. The bromide content in the BMIM4F-Py-COF was measured to be 2.5 wt% (i.e., 0.4 mol%), which means that 42% imidazole moiety was grafted with 1-bromobutane.

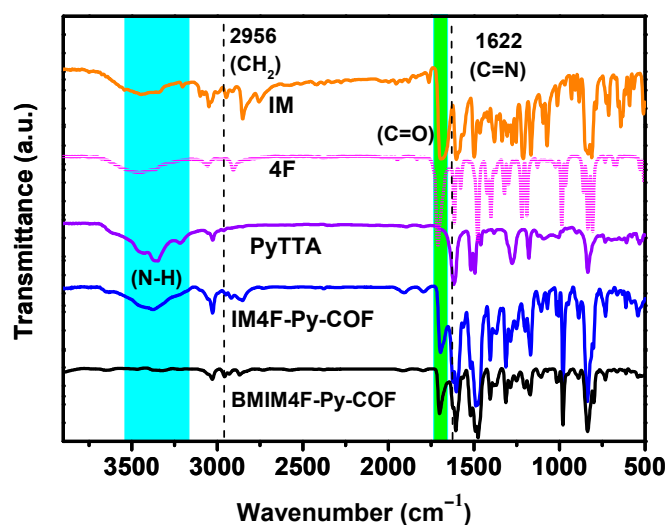


**Figure 2.** FT-IR spectra of IM4F-Py-COF (blue), BMIM4F-Py-COF (black), IM (orange), 4F (magenta) and PyTTA (violet).

The porosity of both COFs was evaluated using nitrogen adsorption–desorption isotherms measured at 77 K. The BET surface areas were estimated to be  $1307\text{ m}^2\text{ g}^{-1}$ , the pore width was calculated to be 3.4 nm and the pore volume was estimated to be  $1.09\text{ cm}^3\text{ g}^{-1}$  for IM4F-Py-COF (Figure 3a). After the modification, the BET surface area, the pore width and the pore volume were slightly decreased to  $865\text{ m}^2\text{ g}^{-1}$ , 3.2 nm and  $1.06\text{ cm}^3\text{ g}^{-1}$ , respectively (Figure 3b), which was ascribed to the introduction of n-butyl within the pores of the IM4F-Py-COF.

The morphology of both COFs was characterized by field-emission scanning electron microscopy (FE-SEM) and high-resolution transmission electron microscopy (HR-TEM). FE-SEM images revealed that IM4F-Py-COF and BMIM4F-Py-COF possessed a lamellar structure several tens of microns in size and with a thickness of hundreds of nanometers (Figure S3). HR-TEM images showed that both COFs had a highly ordered structure, and open channels can be directly observed in Figure 4. Domains oriented along the ab facets perpendicular to the viewing direction showed regular rhombic pores for both COFs (Figure 4a, insert). The results demonstrated the high quality of the COF crystallites. The thermal stabilities of both COFs were also investigated using thermogravimetric analysis (TGA). After modification, the thermal stability of the COF was slightly decreased, although the thermal decomposition temperatures of both COFs were still higher than  $400\text{ }^\circ\text{C}$  (Figure S4), suggesting their good thermal behavior.

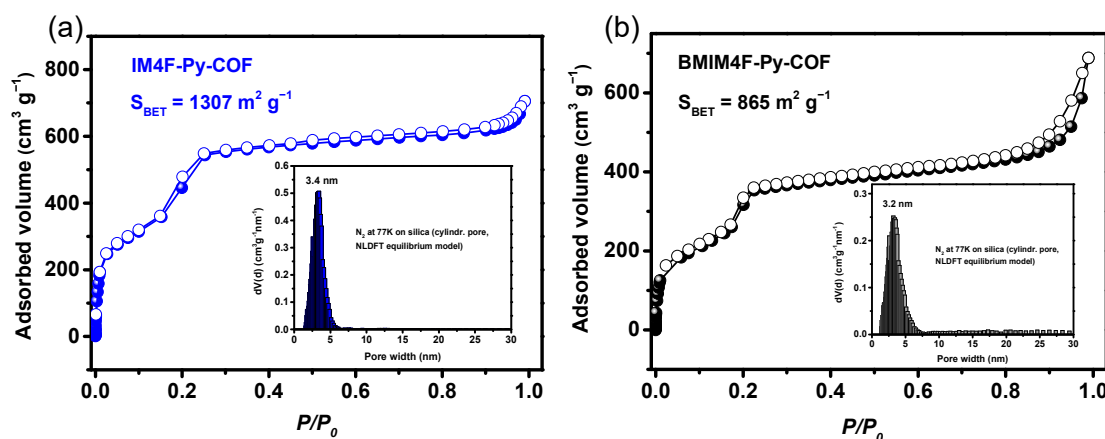


**Figure 3.**  $N_2$  sorption isotherms and pore size distribution (insert) of IM4F-Py-COF (a) and BMIM4F-Py-COF (b).

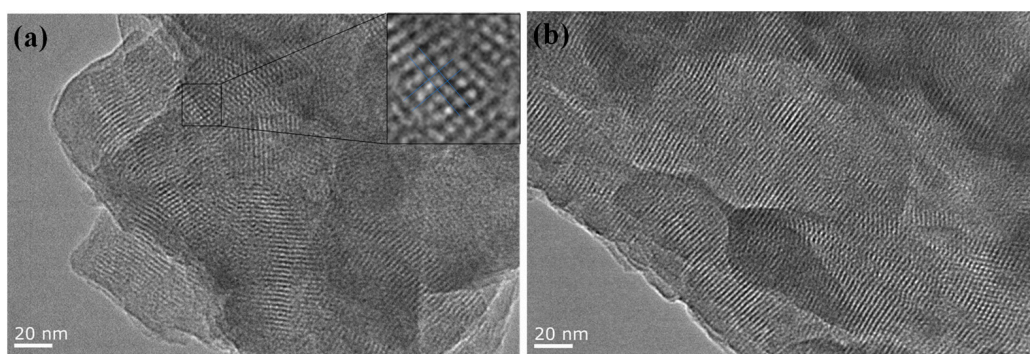


**Figure 4.** FE-TEM images of (a) IM4F-Py-COF and (b) BMIM4F-Py-COF. The inset in Figure 4a shows an enlarged image.

The cycloaddition of  $\text{CO}_2$  to epichlorohydrin was selected as a model reaction in order to establish the activity of the BMIM4F-Py-COF catalyst (Table 1). The reaction mixture was charged in a reactor, which was pressurized with  $\text{CO}_2$  to 4.0 MPa, and reacted at  $110^\circ\text{C}$  for 12 h. Although we aimed to carry out this experiment under milder conditions from an academic perspective, the optimal reaction condition is 4.0–5.0 MPa  $\text{CO}_2$  in practice, due to both material supply and product output issues. Therefore, the  $\text{CO}_2$  pressure was set at the preferred 4.0 MPa in this work. The model reaction produced (chloromethyl)ethylene carbonate in a 97% yield without the use of any solvents (Table 1, entry 1), suggesting an outstanding catalytic performance of BMIM4F-Py-COF. When the amount of BMIM4F-Py-COF catalyst was reduced to half, the yield decreased to 88% (Table 1, entry 2). The effect of temperature and pressure on the product yield was also investigated. In order to compare with our previously reported result [58], the reaction time was set at 24 h here. At this stage, when the temperature was increased from 110 to  $120^\circ\text{C}$ , the BMIM4F-Py-COF demonstrated much better catalytic activity. Even when the pressure of  $\text{CO}_2$  was decreased from 4.0 to 1.0 MPa, the yield of (chloromethyl)ethylene carbonate was still higher than 94% (Table 1, entries 3–6), which is comparable with our previous result [58]. When the reaction time was 12 h, a yield of 91% was observed (Table 1, entry 7), revealing the outstanding catalytic performance of BMIM4F-Py-COF. When the reaction temperature was decreased from 110 to  $90^\circ\text{C}$ , the yield decreased remarkably from 97% to 49% (Table 1, entry 8), suggesting that temperature has a dramatic effect on the yield, in accordance with previously reported results [49,59,60]. Decreasing  $\text{CO}_2$  pressure from 4.0 to 3.0 MPa ( $110^\circ\text{C}$ ) also led to a decreased yield, from 97% to 77% (Table 1, entry 9). The effect of reaction time on the yield was further studied. When the reaction time was shortened from 12 to 10, 8 and 6 h, the yield decreased from 97% to 94%, 92% and 87%, respectively (Table 1,

entry 1 and entries 10–12). When IM4F-Py-COF was used to replace BMIM4F-Py-COF, a yield of only 25% yield was obtained (Table 1, entry 13), suggesting that the reaction was catalyzed by imidazolium bromide active moiety on the BMIM4F-Py-COF.

**Table 1.** Influence of various experimental conditions on cycloaddition reaction <sup>a</sup>.

Entry	Substrate	Catalyst	Pressure	Temperature	Time	Yield <sup>b</sup>	TON <sup>c</sup>
			(MPa)	(°C)	(h)	(%)	
1		BMIM4F-Py-COF	4.0	110	12	97	589
2 <sup>d</sup>		BMIM4F-Py-COF	4.0	110	12	88	1068
3		BMIM4F-Py-COF	4.0	120	24	99	601
4		BMIM4F-Py-COF	3.0	120	24	99	601
5		BMIM4F-Py-COF	2.0	120	24	97	589
6		BMIM4F-Py-COF	1.0	120	24	94	571
7		BMIM4F-Py-COF	1.0	120	12	91	553
8		BMIM4F-Py-COF	4.0	90	12	49	298
9		BMIM4F-Py-COF	3.0	110	12	77	467
10		BMIM4F-Py-COF	4.0	110	10	94	571
11		BMIM4F-Py-COF	4.0	110	8	92	558
12		BMIM4F-Py-COF	4.0	110	6	87	528
13		IM4F-Py-COF	4.0	110	12	25	152

<sup>a</sup> Reaction conditions: epoxide (3.8 mmol), BMIM4F-Py-COF (20 mg, ion content: 0.006 mmol), no additional solvent. <sup>b</sup> Product yield was analyzed using gas chromatography (GC). <sup>c</sup> TON: moles of synthesized cyclic carbonate per mole of imidazolium salt. <sup>d</sup> 10 mg BMIM4F-Py-COF was used as a catalyst.

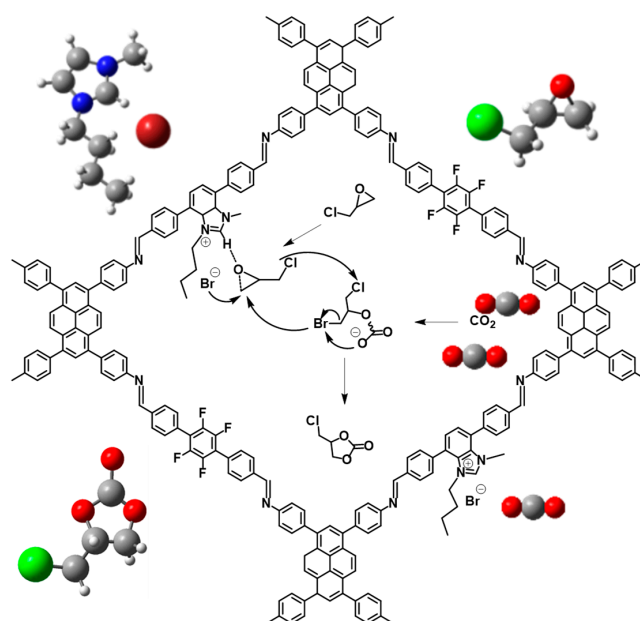
The catalytic activity of BMIM4F-Py-COF in the cycloaddition of CO<sub>2</sub> to different epoxides was investigated under identical conditions (Table 2). When propylene oxide was used as an epoxide, a yield as high as 100% was observed (Table 2, entry 1), which is even higher than that of epichlorohydrin (Table 2, entry 2), and is also consistent with previous reports [61–65]. In addition, the cycloaddition of CO<sub>2</sub> to 1,2-epoxyhexane, 1,2-epoxyoctane, butyl glycidyl ether, 3,4-epoxy-1-butene and styrene oxide was also observed (Table 2, entry 3–7). The yield was 97%, 87%, 85%, 88% and 80%, respectively. From the results, it seems that BMIM4F-Py-COF was more effective for small-size substrates [49,59–65]. We believe that the high catalytic activity of the ionic liquid, the large surface area and the 1D channel walls of the COF may contribute to the excellent catalytic ability of BMIM4F-Py-COF. Although it may seem counter-intuitive to compare the catalytic performance of BMIM4F-Py-COF with other reports because the cycloaddition reactions involve several reaction conditions (e.g., reaction temperature, pressure of CO<sub>2</sub>, solvent, reaction time and dosage of catalyst), we have nonetheless listed a summary of the previously reported catalytic performances of the cycloaddition of CO<sub>2</sub> to epichlorohydrin (Table S2). In line with the data listed in Table S2, we believe that BMIM4F-Py-COF is a valuable heterogeneous catalyst for cycloaddition reactions, especially considering that the reactions were carried out under solvent-free and co-catalyst-free conditions.

**Table 2.** Cycloaddition reactions of CO<sub>2</sub> with various epoxides using BMIM4F-Py-COF as catalyst <sup>a</sup>.

Entry	Substrate	Catalyst	Pressure	Temperature	Time	Yield <sup>b</sup>	TON <sup>c</sup>
			(MPa)	(°C)		(h)	
1		BMIM4F-Py-COF	4.0	110	12	100	608
2		BMIM4F-Py-COF	4.0	110	12	97	589
3		BMIM4F-Py-COF	4.0	90	12	97	589
4		BMIM4F-Py-COF	4.0	110	12	87	529
5		BMIM4F-Py-COF	4.0	110	12	85	517
6		BMIM4F-Py-COF	4.0	110	12	88	535
7		BMIM4F-Py-COF	4.0	110	12	80	486

<sup>a</sup> Reaction conditions: epoxide (3.8 mmol), BMIM4F-Py-COF (20 mg, ion content: 0.006 mmol), no additional solvent. <sup>b</sup> Product yield was analyzed using gas chromatography (GC). <sup>c</sup> TON: moles of synthesized cyclic carbonate per mole of imidazolium salt.

We consider that the reaction is initiated by binding the O atom of the epoxides with the acidic C<sub>2</sub>-proton of the imidazolium cation, through which process the C-O bond of the epoxides is weakened. Subsequently, the Br<sup>-</sup> attacks the less-hindered carbon atom of the coordinated epoxide to open the epoxy ring. Subsequently, CO<sub>2</sub> interacts with the oxygen anion of the opened epoxy ring to form an alkylcarbonate anion, after which a ring closure step gives the cyclic carbonate products (Figure 5) [60–66].

**Figure 5.** Scheme of possible catalytic mechanism for the reaction of epoxides and CO<sub>2</sub> into cyclic carbonates catalyzed by BMIM4F-Py-COF.

The heterogeneity of the BMIM4F-Py-COF catalyst was investigated by removing the catalyst by centrifugation during an ongoing reaction. Without the catalyst, the conversion stopped, and no significant product formation could be observed. The reusability of the BMIM4F-Py-COF and reproducibility of catalytic performance were investigated based on the experimental results of repeated cyclic tests. In each cycle, BMIM4F-Py-COF was removed by centrifugation and then rinsed with epichlorohydrin. After drying, the catalyst was reused for the next run. The yields of cyclic carbonates in the first four consecutive runs are shown in Figure 6. The results indicated that the catalytic activity of BMIM4F-Py-COF could be retained for up to five cycloaddition series. After five runs, no obvious change was found for the PXRD pattern of BMIM4F-Py-COF before and after the catalysis (Figure S5). In addition, no change was observed for the FT-IR spectrum of BMIM4F-Py-COF after five runs (Figure S6). These results reveal that the BMIM4F-Py-COF can thus be considered a renewable and stable catalyst for the cycloaddition of CO<sub>2</sub> to epoxides.

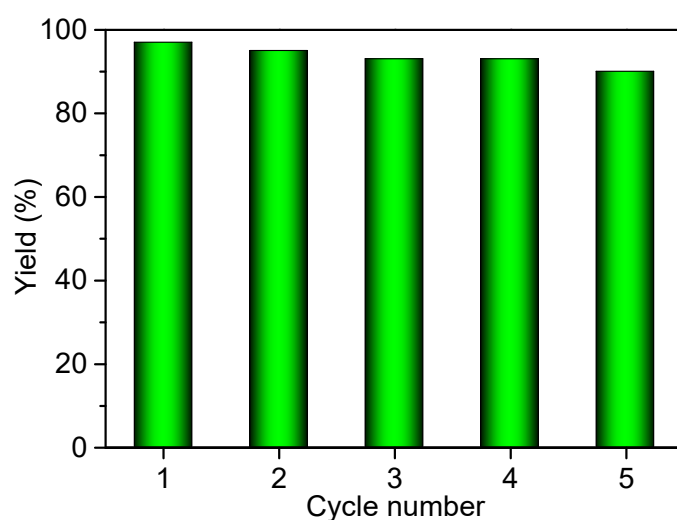


**Figure 6.** Catalytic activity of recycled BMIM4F-Py-COF for cycloaddition of CO<sub>2</sub> to epichlorohydrin.

#### 4. Conclusions

In summary, an ionic BMIM4F-Py-COF was successfully synthesized by grafting an ionic liquid precursor onto the skeleton of a two-dimensional covalent organic framework (2D COF), followed by the ionization of the precursor through the quaternization reaction. The resulting BMIM4F-Py-COF was used as a heterogeneous catalyst for the cycloaddition of CO<sub>2</sub> to epoxides. It was shown that this ionized porous COF showed good catalytic activity even in a solvent- and co-catalyst-free environment. Furthermore, the BMIM4F-Py-COF was continually recycled five times after easy separation without decreasing its activity or selectivity under equivalent reaction conditions. The high catalytic activity of the ionic liquid, a large surface area and the 1D channel walls of the COF were considered to contribute to the excellent catalytic performance of BMIM4F-Py-COF.

**Supplementary Materials:** The following supporting information can be downloaded at: <https://www.mdpi.com/article/10.3390/molecules27196204/s1>, Figure S1: PXRD pattern of BMIM4F-Py-COF. Experimental pattern (black) and AA-stacking (blue); Figure S2: Solid-state <sup>13</sup>C NMR spectra of IM4F-Py-COF (blue) and BMIM4F-Py-COF (black); Figure S3: FE-SEM images of IM4F-Py-COF (a,b) and BMIM4F-Py-COF (c,d); Figure S4: Thermogravimetric analysis of IM4F-Py-COF (blue) and BMIM4F-Py-COF (black); Figure S5: Comparison of PXRD pattern of BMIM4F-Py-COF before (black) and after catalysis (red). The insert indicates an enlarged PXRD pattern; Figure S6: Comparison of FT-IR spectroscopy of BMIM4F-Py-COF before (black) and after catalysis (red); Table S1: Fractional atomic coordinates for the unit cell of IM4F-Py-COF; References citation of [55,56]. Table S2: Comparison with various metal-free catalysts in the performance of the cycloaddition of CO<sub>2</sub> to epichlorohydrin. References [58,67–87] are cited in the supplementary materials.

**Author Contributions:** Conceptualization, X.S. and Y.G.; methodology, Q.Y., F.L. and H.L.; software, H.H.; validation, Q.Y., H.L. and S.W.; formal analysis, Q.Y. and X.J.; investigation, Q.Y., H.X. and X.S.; resources, X.S., S.X. and Y.G.; data curation, Q.Y., F.L. and H.X.; writing—original draft preparation, Y.G.; writing—review and editing, S.X. and Y.G.; visualization, Y.G.; supervision, Y.G.; project administration, Y.G.; funding acquisition, X.S., S.X. and Y.G. All authors have read and agreed to the published version of the manuscript.

**Funding:** This work was supported by the National Natural Science Foundation of China (21965011, 22165009 and 22105053), the Major Science and Technology Plan of Hainan Province (ZDKJ202016), the Natural Science Foundation of Hainan Province (220RC458, 220QN281 and 521QN209) and the Scientific Research Foundation of the Higher Education Institutions of Hainan Province (Hnky2021ZD-22). S.X. would like to thank the Continuous-Support Basic Scientific Research Project, China, for their financial support.

**Institutional Review Board Statement:** Not applicable.

**Informed Consent Statement:** Not applicable.

**Data Availability Statement:** Not applicable.

**Conflicts of Interest:** The authors declare no conflict of interest.

**Sample Availability:** Samples of the building units, IM4F-Py-COF and BMIM4F-Py-COF... are available from the authors.

## References

1. Feng, X.; Ding, X.S.; Jiang, D.L. Covalent organic frameworks. *Chem. Soc. Rev.* **2012**, *41*, 6010–6022. [[CrossRef](#)] [[PubMed](#)]
2. Hu, H.; Yan, Q.Q.; Ge, R.L.; Gao, Y.A. Covalent organic frameworks as heterogeneous catalysts. *Chin. J. Catal.* **2018**, *39*, 1167–1179. [[CrossRef](#)]
3. Geng, K.; He, T.; Liu, R.Y.; Dalapati, S.; Tan, K.T.; Li, Z.P.; Tao, S.S.; Gong, Y.F.; Jiang, Q.H.; Jiang, D.L. Covalent organic frameworks: Design, synthesis, and functions. *Chem. Rev.* **2020**, *120*, 8814–8933. [[CrossRef](#)]
4. Chen, X.Y.; Geng, K.; Liu, R.Y.; Tan, K.T.; Gong, Y.F.; Li, Z.P.; Tao, S.S.; Jiang, Q.H.; Jiang, D.L. Kovalente organische Gerüstverbindungen: Chemische Ansätze für Designerstrukturen und integrierte Funktionen. *Angew. Chem. Int. Ed.* **2020**, *132*, 5086–5129. [[CrossRef](#)]
5. Lin, S.; Diercks, C.S.; Zhang, Y.B.; Kornienko, N.; Nichols, E.M.; Zhao, Y.; Paris, A.R.; Kim, D.; Yang, P.; Yaghi, O.M. Covalent organic frameworks comprising cobalt porphyrins for catalytic CO<sub>2</sub> reduction in water. *Science* **2015**, *349*, 1208–1213. [[CrossRef](#)] [[PubMed](#)]
6. Ding, S.Y.; Gao, J.; Wang, Q.; Zhang, Y.; Song, W.G.; Su, C.Y.; Wang, W. Construction of covalent organic framework for catalysis: Pd/COF-LZU1 in Suzuki-Miyaura coupling reaction. *J. Am. Chem. Soc.* **2011**, *133*, 19816–19822. [[CrossRef](#)]
7. Vyas, V.S.; Haase, F.; Stegbauer, L.; Savasci, G.; Podjaski, F.; Ochsenfeld, C.; Lotsch, B.V. A tunable azine covalent organic framework platform for visible light-induced hydrogen generation. *Nat. Commun.* **2015**, *6*, 8508. [[CrossRef](#)]
8. Sun, Q.; Aguila, B.; Perman, J.; Nguyen, N.; Ma, S. Flexibility matters: Cooperative active sites in covalent organic framework and threaded ionic polymer. *J. Am. Chem. Soc.* **2016**, *138*, 15790–15796. [[CrossRef](#)]
9. Wang, X.; Han, X.; Zhang, J.; Wu, X.; Liu, Y.; Cui, Y. Homochiral 2D porous covalent organic frameworks for heterogeneous asymmetric catalysis. *J. Am. Chem. Soc.* **2016**, *138*, 12332–12335. [[CrossRef](#)]
10. Sun, Q.; Tang, Y.; Aguila, B.; Wang, S.; Xiao, F.S.; Thallapally, P.K.; Al-Enizi, A.M.; Nafady, A.; Ma, S. Reaction environment modification in covalent organic frameworks for catalytic performance enhancement. *Angew. Chem. Int. Ed.* **2019**, *58*, 8670–8675. [[CrossRef](#)]
11. Bhadra, M.; Kandambeth, S.; Sahoo, M.K.; Addicoat, M.; Balaraman, E.; Banerjee, R. Triazine functionalized porous covalent organic framework for photo-organocatalytic E-Z isomerization of olefins. *J. Am. Chem. Soc.* **2019**, *141*, 6152–6156. [[CrossRef](#)] [[PubMed](#)]
12. Du, Y.; Yang, H.; Whiteley, J.M.; Wan, S.; Jin, Y.; Lee, S.H.; Zhang, W. Ionic covalent organic frameworks with spiroborate linkage. *Angew. Chem. Int. Ed.* **2016**, *55*, 1737–1741. [[CrossRef](#)] [[PubMed](#)]
13. Zeng, Y.; Zou, R.; Zhao, Y. Covalent organic frameworks for CO<sub>2</sub> capture. *Adv. Mater.* **2016**, *28*, 2855–2873. [[CrossRef](#)]
14. Baldwin, L.A.; Crowe, J.W.; Pyles, D.A.; McGrier, P.L. Metalation of a mesoporous three-dimensional covalent organic framework. *J. Am. Chem. Soc.* **2016**, *138*, 15134–15137. [[CrossRef](#)] [[PubMed](#)]
15. Pramudya, Y.; Mendoza-Cortes, J.L. Design principles for high H<sub>2</sub> storage using chelation of abundant transition metals in covalent organic frameworks for 0–700 bar at 298 K. *J. Am. Chem. Soc.* **2016**, *138*, 15204–15213. [[CrossRef](#)]
16. Huang, N.; Krishna, R.; Jiang, D.L. Tailor-made pore surface engineering in covalent organic frameworks: Systematic functionalization for performance screening. *J. Am. Chem. Soc.* **2015**, *137*, 7079–7082. [[CrossRef](#)]

17. Lei, Z.; Yang, Q.; Xu, Y.; Guo, S.; Sun, W.; Liu, H.; Lv, L.P.; Zhang, Y.; Wang, Y. Boosting lithium storage in covalent organic framework via activation of 14-electron redox chemistry. *Nat. Commun.* **2018**, *9*, 576. [[CrossRef](#)]
18. Talapaneni, S.N.; Hwang, T.H.; Je, S.H.; Buyukcakir, O.; Choi, J.W.; Coskun, A. Elemental-sulfur-mediated facile synthesis of a covalent triazine framework for high-performance lithium-sulfur batteries. *Angew. Chem. Int. Ed.* **2016**, *55*, 3106–3111. [[CrossRef](#)]
19. Zu, C.; Manthiram, A. Hydroxylated graphene-sulfur nanocomposites for high-rate lithium-sulfur batteries. *Adv. Energy Mater.* **2013**, *3*, 1008–1012. [[CrossRef](#)]
20. Sun, Q.; Aguila, B.; Perman, J.; Earl, L.D.; Abney, C.W.; Cheng, Y.; Wei, H.; Nguyen, N.; Wojtas, L.; Ma, S. Postsynthetically modified covalent organic frameworks for efficient and effective mercury removal. *J. Am. Chem. Soc.* **2017**, *139*, 2786–2793. [[CrossRef](#)]
21. Huang, N.; Zhai, L.; Xu, H.; Jiang, D.L. Stable covalent organic frameworks for exceptional mercury removal from aqueous solutions. *J. Am. Chem. Soc.* **2017**, *139*, 2428–2434. [[CrossRef](#)] [[PubMed](#)]
22. Ding, S.Y.; Dong, M.; Wang, Y.W.; Chen, Y.T.; Wang, H.Z.; Su, C.Y.; Wang, W. Thioether-based fluorescent covalent organic framework for selective detection and facile removal of mercury (II). *J. Am. Chem. Soc.* **2016**, *138*, 3031–3037. [[CrossRef](#)] [[PubMed](#)]
23. Mellah, A.; Fernandes, S.P.; Rodríguez, R.; Otero, J.; Paz, J.; Cruces, J.; Medina, D.D.; Djamila, H.; Espiña, B.; Salonen, L.M. Adsorption of pharmaceutical pollutants from water using covalent organic frameworks. *Chem. Eur. J.* **2018**, *24*, 10601–10605. [[CrossRef](#)] [[PubMed](#)]
24. Sun, Q.; Aguila, B.; Earl, L.D.; Abney, C.W.; Wojtas, L.; Thallapally, P.K.; Ma, S. Covalent organic frameworks as a decorating platform for utilization and affinity enhancement of chelating sites for radionuclide sequestration. *Adv. Mater.* **2018**, *30*, 1705479–1705487. [[CrossRef](#)]
25. Rogge, S.M.; Bavykina, A.; Hajek, J.; Garcia, H.; Olivos-Suarez, A.I.; Sepúlveda-Escribano, A.; Vimont, A.; Clet, G.; Bazin, P.; Kapteijn, F. Metal-organic and covalent organic frameworks as single-site catalysts. *Chem. Soc. Rev.* **2017**, *46*, 3134–3184. [[CrossRef](#)]
26. Xu, H.; Gao, J.; Jiang, D.L. Stable, crystalline, porous, covalent organic frameworks as a platform for chiral organocatalysts. *Nat. Chem.* **2015**, *7*, 905–912. [[CrossRef](#)]
27. Zhang, J.Q.; Peng, Y.S.; Leng, W.G.; Gao, Y.A.; Xu, F.F.; Chai, J.L. Nitrogen ligands in two-dimensional covalent organic frameworks for metal catalysis. *Chin. J. Catal.* **2016**, *37*, 468–475. [[CrossRef](#)]
28. Xu, H.; Chen, X.; Gao, J.; Lin, J.B.; Addicoat, M.; Irle, S.; Jiang, D.L. Catalytic covalent organic frameworks via pore surface engineering. *Chem. Commun.* **2014**, *50*, 1292–1294. [[CrossRef](#)]
29. Li, L.H.; Feng, X.L.; Cui, X.H.; Ma, Y.X.; Ding, S.Y.; Wang, W. Salen-based covalent organic framework. *J. Am. Chem. Soc.* **2017**, *139*, 6042–6045. [[CrossRef](#)]
30. Wu, Y.; Xu, H.; Chen, X.; Gao, J.; Jiang, D.L. A  $\pi$ -electronic covalent organic framework catalyst:  $\pi$ -walls as catalytic beds for Diels-Alder reactions under ambient conditions. *Chem. Commun.* **2015**, *51*, 10096–10098. [[CrossRef](#)]
31. Leng, W.G.; Ge, R.L.; Dong, B.; Wang, C.; Gao, Y.A. Bimetallic docked covalent organic frameworks with high catalytic performance towards tandem reactions. *RSC Adv.* **2016**, *6*, 37403–37406. [[CrossRef](#)]
32. Sun, Q.; Aguila, B.; Ma, S. A bifunctional covalent organic framework as an efficient platform for cascade catalysis. *Mater. Chem. Front.* **2017**, *1*, 1310–1316. [[CrossRef](#)]
33. Leng, W.G.; Peng, Y.S.; Zhang, J.Q.; Lu, H.; Feng, X.; Ge, R.L.; Dong, B.; Wang, B.; Hu, X.P.; Gao, Y.A. Sophisticated design of covalent organic frameworks with controllable bimetallic docking for a cascade reaction. *Chem. Eur. J.* **2016**, *22*, 9087–9091. [[CrossRef](#)] [[PubMed](#)]
34. Liu, J.; Thallapally, P.K.; McGrail, B.P.; Brown, D.R.; Liu, J. Progress in adsorption-based CO<sub>2</sub> capture by metal-organic frameworks. *Chem. Soc. Rev.* **2012**, *41*, 2308–2322. [[CrossRef](#)]
35. Yoshida, M.; Ihara, M. Novel methodologies for the synthesis of cyclic carbonates. *Chem. Eur. J.* **2004**, *10*, 2886–2893. [[CrossRef](#)] [[PubMed](#)]
36. Dai, W.L.; Luo, S.L.; Yin, S.F.; Au, C.T. The direct transformation of carbon dioxide to organic carbonates over heterogeneous catalysts. *Appl. Catal. A Gen.* **2009**, *366*, 2–12. [[CrossRef](#)]
37. Sakakura, T.; Kohno, K. The synthesis of organic carbonates from carbon dioxide. *Chem. Commun.* **2009**, *11*, 1312–1330. [[CrossRef](#)]
38. Shen, Y.M.; Duan, W.L.; Shi, M. Chemical fixation of carbon dioxide co-catalyzed by a combination of Schiff bases or phenols and organic bases. *Eur. J. Org. Chem.* **2004**, *14*, 3080–3089. [[CrossRef](#)]
39. Zhou, F.; Xie, S.L.; Gao, X.T.; Zhang, R.; Wang, C.H.; Yin, G.Q.; Zhou, J. Activation of (salen)CoI complex by phosphorane for carbon dioxide transformation at ambient temperature and pressure. *Green Chem.* **2017**, *19*, 3908–3915. [[CrossRef](#)]
40. Ema, T.; Miyazaki, Y.; Shimonishi, J.; Maeda, C.; Hasegawa, J. Bifunctional porphyrin catalysts for the synthesis of cyclic carbonates from epoxides and CO<sub>2</sub>: Structural optimization and mechanistic study. *J. Am. Chem. Soc.* **2014**, *136*, 15270–15279. [[CrossRef](#)]
41. Sun, J.; Zhang, S.; Cheng, W.; Ren, J. Hydroxyl-functionalized ionic liquid: A novel efficient catalyst for chemical fixation of CO<sub>2</sub> to cyclic carbonate. *Tetrahedron Lett.* **2008**, *49*, 3588–3591. [[CrossRef](#)]
42. Caló, V.; Nacci, A.; Monopoli, A.; Fanizzi, A. Cyclic carbonate formation from carbon dioxide and oxiranes in tetrabutylammonium halides as solvents and catalysts. *Org. Lett.* **2002**, *4*, 2561–2563. [[CrossRef](#)] [[PubMed](#)]

43. Sun, J.M.; Fujita, S.; Arai, M. Development in the green synthesis of cyclic carbonate from carbon dioxide using ionic liquids. *J. Organomet. Chem.* **2005**, *690*, 3490–3497. [[CrossRef](#)]
44. Peng, J.; Deng, Y. Cycloaddition of carbon dioxide to propylene oxide catalyzed by ionic liquids. *New J. Chem.* **2001**, *25*, 639–641. [[CrossRef](#)]
45. Kawanami, H.; Sasaki, A.; Matsui, K.; Ikushima, Y. A rapid and effective synthesis of propylene carbonate using a supercritical CO<sub>2</sub>-ionic liquid system. *Chem. Commun.* **2003**, 896–897. [[CrossRef](#)] [[PubMed](#)]
46. Yang, H.; Gu, Y.; Deng, Y.; Shi, F. Electrochemical activation of carbon dioxide in ionic liquid: Synthesis of cyclic carbonates at mild reaction conditions. *Chem. Commun.* **2002**, 274–275. [[CrossRef](#)]
47. Han, L.; Choi, H.J.; Choi, S.J.; Liu, B.; Park, D.W. Ionic liquids containing carboxyl acid moieties grafted onto silica: Synthesis and application as heterogeneous catalysts for cycloaddition reactions of epoxide and carbon dioxide. *Green Chem.* **2011**, *13*, 1023–1028. [[CrossRef](#)]
48. Han, L.; Park, S.W.; Park, D.W. Silica grafted imidazolium-based ionic liquids: Efficient heterogeneous catalysts for chemical fixation of CO<sub>2</sub> to a cyclic carbonate. *Energy Environ. Sci.* **2009**, *2*, 1286–1292. [[CrossRef](#)]
49. Xie, Y.; Zhang, Z.F.; Jiang, T.; He, J.L.; Han, B.X.; Wu, T.B.; Ding, K.L. CO<sub>2</sub> cycloaddition reactions catalyzed by an ionic liquid grafted onto a highly cross-linked polymer matrix. *Angew. Chem. Int. Ed.* **2007**, *46*, 7255–7258. [[CrossRef](#)]
50. Tharun, J.; Bhin, K.M.; Roshan, R.; Kim, D.W.; Kathalikkattil, A.C.; Babu, R.; Ahn, H.Y.; Won, Y.S.; Park, D.W. Ionic liquid tethered post functionalized ZIF-90 framework for the cycloaddition of propylene oxide and CO<sub>2</sub>. *Green Chem.* **2016**, *18*, 2479–2487. [[CrossRef](#)]
51. Ma, H.P.; Liu, B.; Li, B.; Zhang, L.; Li, Y.G.; Tan, H.Q.; Zang, H.Y.; Zhu, G.S. Cationic covalent organic frameworks: A simple platform of anionic exchange for porosity tuning and proton conduction. *J. Am. Chem. Soc.* **2016**, *138*, 5897–5903. [[CrossRef](#)] [[PubMed](#)]
52. Dong, B.; Wang, L.Y.; Zhao, S.; Ge, R.L.; Song, X.D.; Wang, Y.; Gao, Y.A. Immobilization of ionic liquids to covalent organic frameworks for catalyzing the formylation of amines with CO<sub>2</sub> and phenylsilane. *Chem. Commun.* **2016**, *52*, 7082–7085. [[CrossRef](#)] [[PubMed](#)]
53. Hu, H.; Yan, Q.Q.; Wang, M.; Yu, L.; Pan, W.; Wang, B.S.; Gao, Y.A. Ionic covalent organic frameworks for highly effective catalysis. *Chin. J. Catal.* **2018**, *39*, 1437–1444. [[CrossRef](#)]
54. Huang, N.; Wang, P.; Addicoat, M.A.; Heine, T.; Jiang, D.L. Ionic covalent organic frameworks: Design of a charged interface aligned on 1D channel walls and its unusual electrostatic functions. *Angew. Chem. Int. Ed.* **2017**, *56*, 4982–4986. [[CrossRef](#)] [[PubMed](#)]
55. Kuhnert, N.; Patel, C.; Jami, F. Synthesis of chiral nonracemic polyimine macrocycles from cyclocondensation reactions of biaryl and terphenyl aromatic dicarboxaldehydes and 1R, 2R-diaminocyclohexane. *Tetrahedron Lett.* **2005**, *46*, 7575–7579. [[CrossRef](#)]
56. Chai, Y.Y.; Li, Y.L.; Hu, H.; Zeng, C.Y.; Wang, S.L.; Xu, H.J.; Gao, Y.A. N-Heterocyclic Carbene Functionalized Covalent Organic Framework for Transesterification of Glycerol with Dialkyl Carbonates. *Catalysts* **2021**, *11*, 423. [[CrossRef](#)]
57. Chen, X.; Addicoat, M.; Irle, S.; Nagai, A.; Jiang, D.L. Control of crystallinity and porosity of covalent organic frameworks by managing interlayer interactions based on self-complementary  $\pi$ -electronic force. *J. Am. Chem. Soc.* **2013**, *135*, 546–549. [[CrossRef](#)]
58. Zhang, Y.; Hu, H.; Ju, J.; Yan, Q.Q.; Arumugam, V.; Jing, X.C.; Cai, H.Q.; Gao, Y.A. Ionization of a covalent organic framework for catalyzing the cycloaddition reaction between epoxides and carbon dioxide. *Chin. J. Catal.* **2020**, *41*, 485–493. [[CrossRef](#)]
59. Maeda, C.; Taniguchi, T.; Ogawa, K.; Ema, T. Bifunctional Catalysts Based on *m*-Phenylene-Bridged Porphyrin Dimer and Trimer Platforms: Synthesis of Cyclic Carbonates from Carbon Dioxide and Epoxides. *Angew. Chem. Int. Ed.* **2015**, *54*, 134–138. [[CrossRef](#)]
60. Chen, J.; Zhong, M.M.; Tao, L.; Liu, L.N.; Jayakumar, S.; Li, C.Z.; Li, H.; Yang, Q.H. The cooperation of porphyrin-based porous polymer and thermal-responsive ionic liquid for efficient CO<sub>2</sub> cycloaddition reaction. *Green Chem.* **2018**, *20*, 903–911. [[CrossRef](#)]
61. Maeda, C.; Shimonishi, J.; Miyazaki, R.; Hasegawa, J.; Ema, T. Highly active and robust metalloporphyrin catalysts for the synthesis of cyclic carbonates from a broad range of epoxides and carbon dioxide. *Chem. Eur. J.* **2016**, *22*, 6556–6563. [[CrossRef](#)] [[PubMed](#)]
62. Feng, D.; Chung, W.C.; Wei, Z.; Gu, Z.Y.; Jiang, H.L.; Chen, Y.P.; Darenbourg, D.J.; Zhou, H.C. Construction of ultrastable porphyrin Zr metal-organic frameworks through linker elimination. *J. Am. Chem. Soc.* **2013**, *135*, 17105–17110. [[CrossRef](#)] [[PubMed](#)]
63. Gao, W.Y.; Chen, Y.; Niu, Y.; Williams, K.; Cash, L.; Perez, P.J.; Wojtas, L.; Cai, J.; Chen, Y.S.; Ma, S. Crystal engineering of an nbo topology metal-organic framework for chemical fixation of CO<sub>2</sub> under ambient conditions. *Angew. Chem. Int. Ed.* **2014**, *53*, 2615–2619. [[CrossRef](#)] [[PubMed](#)]
64. Wu, G.P.; Ren, W.M.; Luo, Y.; Li, B.; Zhang, W.Z.; Lu, X.B. Enhanced asymmetric induction for the copolymerization of CO<sub>2</sub> and cyclohexene oxide with unsymmetric enantiopure salenCo(III) complexes: Synthesis of crystalline CO<sub>2</sub>-based polycarbonate. *J. Am. Chem. Soc.* **2012**, *134*, 5682–5688. [[CrossRef](#)]
65. Li, P.Z.; Wang, X.J.; Liu, J.; Lim, J.S.; Zou, R.; Zhao, Y. A triazole-containing metal-organic framework as a highly effective and substrate size-dependent catalyst for CO<sub>2</sub> conversion. *J. Am. Chem. Soc.* **2016**, *138*, 2142–2145. [[CrossRef](#)]
66. Li, Y.L.; Zhang, J.Q.; Zuo, K.M.; Li, Z.P.; Wang, Y.; Hu, H.; Zeng, C.Y.; Xu, H.J.; Wang, B.S.; Gao, Y.A. Covalent organic frameworks for simultaneous CO<sub>2</sub> capture and selective catalytic transformation. *Catalysts* **2021**, *11*, 1133. [[CrossRef](#)]
67. Saptal, V.; Shinde, D.B.; Banerjee, R.; Bhanage, B.M. State-of-the-art catechol porphyrin COF catalyst for chemical fixation of carbon dioxide via cyclic carbonates and oxazolidinones. *Catal. Sci. Technol.* **2016**, *6*, 6152–6158. [[CrossRef](#)]

68. Roeser, J.; Kailasam, K.; Thomas, A. Covalent triazine frameworks as heterogeneous catalysts for the synthesis of cyclic and linear carbonates from carbon dioxide and epoxides. *ChemSusChem* **2012**, *5*, 1793–1799. [[CrossRef](#)]
69. Buyukcakir, O.; Je, S.H.; Talapaneni, S.N.; Kim, D.; Coskun, A. Charged Covalent Triazine Frameworks for CO<sub>2</sub> Capture and Conversion. *ACS Appl. Mater. Interfaces* **2017**, *9*, 7209–7216. [[CrossRef](#)]
70. Guo, Z.J.; Cai, X.C.; Xie, J.Y.; Wang, X.C.; Zhou, Y.; Wang, J. Hydroxyl-Exchanged Nanoporous Ionic Copolymer toward Low-Temperature Cycloaddition of Atmospheric Carbon Dioxide into Carbonates. *ACS Appl. Mater. Interfaces* **2016**, *8*, 12812–12821. [[CrossRef](#)]
71. Cai, S.; Zhu, D.L.; Zou, Y.; Zhao, J. Porous polymers bearing functional quaternary ammonium salts as efficient solid catalysts for the fixation of CO<sub>2</sub> into cyclic carbonates. *Nanoscale Res. Lett.* **2016**, *11*, 321. [[CrossRef](#)] [[PubMed](#)]
72. Wang, J.Q.; Sng, W.H.; Yi, G.S.; Zhang, Y.G. Imidazolium salt-modified porous hypercrosslinked polymers for synergistic CO<sub>2</sub> capture and conversion. *Chem. Commun.* **2015**, *51*, 12076–12079. [[CrossRef](#)] [[PubMed](#)]
73. Ding, M.L.; Jiang, H.L. Imidazolium salt-modified porous hypercrosslinked polymers for synergistic CO<sub>2</sub> capture and conversion. *Chem. Commun.* **2016**, *52*, 12294–12297. [[CrossRef](#)] [[PubMed](#)]
74. Wang, T. X.; Mu, Z.J.; Ding, X.S.; Han, B. H. Functionalized COFs with Quaternary Phosphonium Salt for Versatilely Catalyzing Chemical Transformations of CO<sub>2</sub>. *Chem. Res. Chin. Univ.* **2022**, *38*, 446–455. [[CrossRef](#)]
75. Du, Y.R.; Yang, X.; Wang, Y.F.; Guan, P.X.; Wang, R.; Xu, B.H. Immobilization poly(ionic liquid)s into hierarchical porous covalent organic frameworks as heterogeneous catalyst for cycloaddition of CO<sub>2</sub> with epoxides. *Mol. Catal.* **2022**, *520*, 112164. [[CrossRef](#)]
76. Zhang, Y.W.; El-Sayed, E.M.; Su, K.Z.; Yuan, D.Q.; Han, Z.B. Evaluation of CO<sub>2</sub> utilization for methanol production via tri-reforming of methane. *J. CO<sub>2</sub> Util.* **2020**, *42*, 1013.
77. Zhi, Y.; Shao, P.; Feng, X.; Xia, H.; Zhang, Y.; Shi, Z.; Mu, Y.; Liu, X. Covalent organic frameworks: Efficient, metal-free, heterogeneous organocatalysts for chemical fixation of CO<sub>2</sub> under mild conditions. *J. Mater. Chem. A*, **2018**, *6*, 374–382. [[CrossRef](#)]
78. Cao, J.; Shan, W.; Wang, Q.; Ling, X.; Li, G.; Lyu, Y.; Zhou, Y.; Wang, J. Ordered Porous Poly(ionic liquid) Crystallines: Spacing Confined Ionic Surface Enhancing Selective CO<sub>2</sub> Capture and Fixation. *ACS Appl. Mater. Inter.* **2019**, *11*, 6031–6041. [[CrossRef](#)]
79. Ding, L.G.; Yao, B.J.; Li, F.; Shi, S.C.; Huang, N.; Yin, H.B.; Guan, Q.; Dong, Y.B. Ionic liquid-decorated COF and its covalent composite aerogel for selective CO<sub>2</sub> adsorption and catalytic conversion. *J. Mater. Chem. A*. **2019**, *7*, 4689–4698. [[CrossRef](#)]
80. Lei, Y.T.; Gunaratne, H.; Jin, L.L. Design and synthesis of pyridinamide functionalized ionic liquids for efficient conversion of carbon dioxide into cyclic carbonates. *J. CO<sub>2</sub> Util.* **2022**, *58*, 101930. [[CrossRef](#)]
81. Katekomol, P.; Roeser, J.; Bojdys, M.; Weber, J.; Thomas, A. Covalent triazine frameworks prepared from 1, 3, 5-tricyanobenzene. *Chem. Mater.* **2013**, *25*, 1542–1548. [[CrossRef](#)]
82. Yu, W.; Gu, S.; Fu, Y.; Xiong, S.; Pan, C.; Liu, Y.; Yu, G. Carbazole-decorated covalent triazine frameworks: Novel nonmetal catalysts for carbon dioxide fixation and oxygen reduction reaction. *J. Catal.* **2018**, *362*, 1–9. [[CrossRef](#)]
83. Yang, F.; Li, Y.; Zhang, T.; Zhao, Z.; Xing, G.; Chen, L. Docking Site Modulation of Isostructural Covalent Organic Frameworks for CO<sub>2</sub> Fixation. *Chem. Eur. J.* **2020**, *26*, 4510–4514. [[CrossRef](#)]
84. Li, H.; Feng, X.; Shao, P.; Chen, J.; Li, C.; Jayakumar, S.; Yang, Q. Synthesis of covalent organic frameworks via in situ salen skeleton formation for catalytic applications. *J. Mater. Chem. A* **2019**, *7*, 5482–5492. [[CrossRef](#)]
85. Cao, J.; Shan, W.; Wang, Q.; Ling, X.; Li, G.; Lyu, Y.; Zhou, Y.; Wang, J. Zinc 2-N-methyl N-confused porphyrin: An efficient catalyst for the conversion of CO<sub>2</sub> into cyclic carbonates. *ACS Appl. Mater. Interfaces*, **2019**, *11*, 6031–6041. [[CrossRef](#)]
86. Qiu, J.; Zhao, Y.; Li, Z.; Wang, H.; Shi, Y.; Wang, J.J. Imidazolium-Salt-Functionalized Covalent Organic Frameworks for Highly Efficient Catalysis of CO<sub>2</sub> Conversion. *ChemSusChem* **2019**, *12*, 2421–2427.
87. Zhao, Y.; Zhao, Y.; Qiu, J.; Li, Z.; Wang, H.; Wang, J. Facile Grafting of Imidazolium Salt in Covalent Organic Frameworks with Enhanced Catalytic Activity for CO<sub>2</sub> Fixation and the Knoevenagel Reaction. *ACS Sustain. Chem. Eng.* **2020**, *8*, 18413–18419. [[CrossRef](#)]